Journal of Ceramic Processing Research. Vol. 14, No. 3, pp. 349~354 (2013)

J O U R N A L O F
Ceramic Processing Research

Synthesis of CdSe-graphene-TiO_2 composites by a facile hydrothermal method with high photocatalytic performance

Ze-Da Meng[a], Lei Zhu[a], Chang Sung Lim[a], Kefayat Ullah[a], Shu Ye[a], Kwang-Youn Cho[b] and Won-Chun Oh[a,*]
[a]*Department of Advanced Materials Science & Engineering, Hanseo University, Seosan, Chungnam, Korea, 356-706*
[b]*Korea Institute of Ceramic Engineering and Technology, Seoul 153-801, Korea*

Herein we obtained a chemically bonded CdSe-graphene-TiO_2 composites using a facile hydrothermal method. During the hydrothermal reaction, both of the reduction of graphene oxide and loading of CdSe and TiO_2 particles were achieved. The as-prepared CdSe-graphene-TiO_2 composites possessed great adsorptivity of dyes, extended light absorption range, and efficient charge separation properties simultaneously. Hence, in the photodegradation of methylene blue, a significant enhancement in the reaction rate was observed with CdSe-graphene-TiO_2 composites, compared to the pure TiO_2 and CdSe-TiO_2. The high activity can be attributed to the synergetic effects of high charge mobility, and red shift in absorption edge of CdSe-graphene-TiO_2 composites.

Key words: CdSe-graphene-TiO_2 composites, Hydrothermal, UV-vis DRS, Photodegradation.

Introduction

TiO_2 has attracted much attention in last score years not only for its effectiveness as materials for photoelectric conversion and photocatalysis, but also for its inexpensiveness, easy production, photochemical and biological stability, and innocuity to the environment and human beings [1, 2]. However, TiO_2 has a wide energy band gap of 3.2 eV so that it can be excited only by the ultraviolet light which is only about 4-6% of the solar spectrum. So, TiO_2 nanoparticles cannot efficiently utilize the solar energy. In addition, the high recombining probability of electrons and holes photogenerated in TiO_2 would decrease its photocatalytic activity. All these drawbacks limit its application especially in the large-scale industry. To solve the above problems, many methods have been applied to extend the light absorption of TiO_2 into the visible region and increase its photocatalytic activity. Compared with other materials, semiconductors (or quantum dots) have attracted consid-erable interest in the past two decades because of their applications in single electron transistors [3], lasers [4], light emitting diodes [5], and infrared photodetectors [6] operating at lower currents and higher temperatures. Various semiconductors, including CdS [8], PbS [9], Bi_2S_3 [10], CdSe [11, 12], and InP [13], have been investigated to sensitize TiO_2 as a visible light absorber. Among these semiconductors, Cadmium selenide (CdSe) is a kind of semiconductor with forbidden zone of 1.7 eV, and its valence electrons can be easily evoked to conduction band when the light wavelength of evoking light is less than or equal to 730 nm. In addition, CdSe exhibits much greater photostability than organic dyes when used as a photosensitizer.

Graphene-based composite materials have attracted much attention as recent studies have shown their usefulness in electronics, photocatalysis and photovoltaic devices [14-16]. Graphene is able to enhance charge transport in a multitude of devices owing to its unique structure: an abundance of delocalized electrons within its conjugated sp^2-bonded graphitic carbon network enables graphene with excellent conductivity. To date, various metals-RGO and metal oxide-RGO nanocomposites including palladium, silver, gold, TiO_2, and CdSe particles have been reported [17-21]. However, there is no report on the synthesis and utilization of CdSe-graphene-TiO2 photocatalyst systems for environmental purification under visible light irradiation.

In this work, we present our studies on the preparation of CdSe-graphene-TiO_2 composites using a facile one-step hydrothermal method and utilization for photo degradation of methylene blue (MB) aqueous solution under visible light. CdSe-graphene-TiO_2 composites were characterized by X-ray diffraction (XRD), scanning electron microscopy (SEM) with an energy dispersive X-ray (EDX) analysis, UV-vis diffuse reflectance spectra (DRS), transmission electron microscopy (TEM). The reasons for improving the photocatalytic activity of CdSe-graphene-TiO_2 composites were also discussed.

Experimental

Materials

Cadmium acetate dihydrate ($Cd(CH_3COO)_2$, 98%), Selenium (Se) metal powder and ammonium hydroxide

*Corresponding author:
Tel : +82-41-660-1337
Fax: +82-41-688-3352
E-mail: wc_oh@hanseo.ac.kr

(NH_4OH, 28%) were purchased from DaeJung Chemicals & Metal Co., Ltd, Korea. Anhydrous purified sodium sulfite (Na_2SO_3, 95%) was purchased from Duksan Pharmaceutical Co., Ltd, Korea. Titanium oxide nanopowder (TiO_2, < 25 nm, 99.7%) with anatase structure was purchased from Sigma-Aldrich Chemistry, USA. Methylene blue (MB, $C_{16}H_{18}N_3S \cdot Cl$, 99.99+%) was used as model pollutant which purchased from Duksan Pure Chemical Co., Ltd, Korea. All chemicals used without further purification and all experiments were carried out using distilled water.

Synthesis of CdSe-graphene-TiO_2 composites

Firstly, Na_2SO_3 (5 g) and Selenium metal powder (0.5 g) were dissolved in 30 mL distilled water and refluxed for 1 h to form Na_2SeSO_3 solution. And $Cd(CH_3COO)_2$ (0.5 g) was dissolved in 2 mL distilled water. NH_4OH (6 mL) was added to it and the mixture was stirred till it dissolved completely to form $Cd(NH_3)_4^{2+}$ solution. Then the graphene oxide which prepared by a Hummers-Offeman method in our previous work [22-24] and TiO_2 nanopowder were added into Na_2SeSO_3 solution and $Cd(NH_3)_4^{2+}$ solution under stirring to allow formation of hydrogen bands between CdSe nanocrystals, TiO_2 nanopowder and graphene oxide. After a hydrothermal reaction at 80 °C for 5 h, graphene oxide was reduced to graphene nanosheet and CdSe compounds and TiO_2 particles naturally grew on its surface to generate a CdSe-graphene-TiO_2 composites. Finally, after the temperature of the mixture was brought down to room temperature and the mixture was filtered through What-man filter paper. The solid obtained was collected and washed with distill water for 5 times. After being dried in vacuum at 100 °C for 8 h, the CdSe-graphene-TiO_2 composites were obtained. We prepared three kinds of CdSe-graphene-TiO_2 composites by changing the amount of graphene oxide and their nomenclatures are listed in Table 1.

Characterization

X-ray diffraction (XRD, Shimadz XD-D1) result was used to identify the crystallinity with monochromatic high-intensity CuKα radiation (λ = 1.5406 Å). Scanning electron microscopy (SEM, JSM-5600) was used to observe the surface state and structure of prepared composite using an electron microscope. The element mapping over the desired region of prepared composite was detected by an energy dispersive X-ray (EDX) analysis attached to SEM. UV-vis diffuse reflectance spectra (DRS) were obtained using an UV-vis spectrophotometer (Neosys-2000) by using $BaSO_4$ as a reference at room temperature and were converted from reflection to absorbance by the Kubelka-Munk method. TEM was also used to examine the size and distribution of the titanium and iron particles deposited on the fullerene surface of various samples. The TEM specimens were prepared by placing a few drops of the sample solution on a carbon grid.

Table 1. summary of preparation condition and nomenclatures of samples

Preparation condition	Nomenclatures
Graphene (0.02 g) + CdSe + TiO_2	GCST1
Graphene (0.04 g) + CdSe + TiO_2	GCST2
Graphene (0.06 g) + CdSe + TiO_2	GCST3

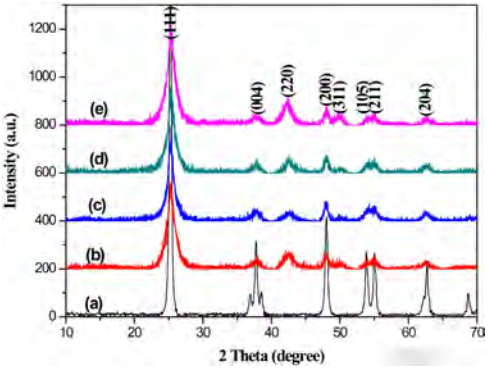

Fig. 1. XRD patterns of pure TiO_2 (a), CdSe-TiO_2 (b), GCST1 (c), GCST2 (d) and GCST3 (e).

Photocatalytic studies

In an ordinary photocatalytic test performed at room temperature, 0.03 g CdSe-graphene-TiO_2 composites were added into 50 mL of 5.0×10^{-5} mol/L MB solution and maintained in dark. After maintaining continuously in the dark for 2 h to ensure establishment of adsorption/desorption equilibrium of organic dyes. Then, the solution was irradiated with visible lamp (8W, λ = 420 nm). The first sample was taken out at the end of the dark adsorption period (just before the light was turned on), in order to determine the MB concentration in solution after dark adsorption, it was treated as the starting point ($t = 0$) of the reaction, where the concentration of MB solution was considered as c_0. Samples were then withdrawn regularly from the reactor by an order of 30 min, 60 min, 90 min, 120 min, 180 min and 240 min, and immediately centrifuged to separate any suspended solid before analysis. The concentration of MB solution (c) during the photocatalytic degradation reaction was monitored through measuring the absorbance of the solution samples with UV-vis spectrophotometer (Optizen POP) at $\lambda_{max} = 665$ nm of MB by using a calibration curve since no reaction by products absorb at these wavelength.

Results and Discussion

Characterization

XRD analysis was used to determine the phase purity and the average crystalline properties of CdSe-graphene-TiO_2 composites. Fig. 1 shows the XRD patterns of pure TiO_2, CdSe-TiO_2 and resulting CdSe-

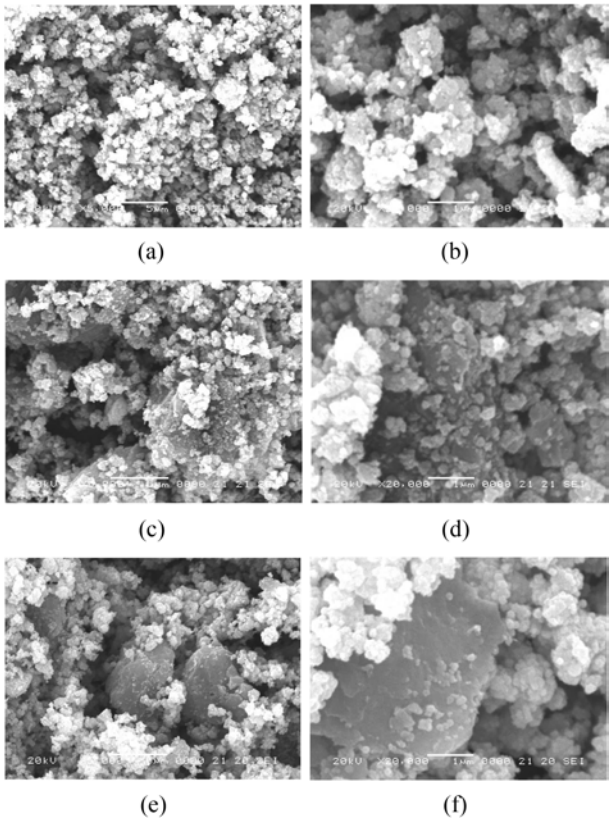

Fig. 2. SEM morphology of CdSe-graphene-TiO_2 composites; GCST1 (a and b), GCST2 (c and d) and GCST3 (e and f).

graphene-TiO_2 composites. Comparison with the patterns of pure TiO_2, the XRD diffraction peaks around 2θ of 37.9 °, 47.8 °, 54.3 °, 55 ° and 62.7 °, which could be indexed to the characteristic peaks (004), (200), (105), (211) and (204) of anatase TiO_2 (JCPDS No. 21-1272) [25], can be observed in all of CdSe-graphene-TiO_2 composites. There no peaks around of 27.4 °, 36.1 °, 41.2 ° and 54.3 ° belong to the diffraction peaks of (110), (101), (111) and (211) of rutile (JCPDS No. 21-1276) [26]. It can be indicated that the anatase form is dominant in all of the CdSe-graphene-TiO_2 composites prepared through the solvethermal process. Some peaks around 2θ of 25.4 °, 42 ° and 49.6 °, which could be indexed to the characteristic peaks (111), (220), and (311) plane reflections of cubic crystal structure CdSe with lattice constants of 6.05 Å (JCPDS No. 65-2891) [27, 28] are also exited in the XRD patterns of CdSe-graphene-TiO_2 composites. There is no change obviously with increasing original amount of graphene from 0.02 g to 0.06 g. However, it shows an evident change of the characteristic peak width and intensity. Notably, the intensity of significant peaks of CdSe is increased with increasing of amount of graphene, indicate more extended crystallized domains of CdSe on the surface of graphene.

Fig. 2 shows the morphology of CdSe-graphene-TiO_2 composites under a SEM microscope. The morphological features of all samples are essentially identical, except

Table 2. EDX elemental microanalysis (wt. %) of CdSe-graphene-TiO_2 composites

Samples	Elements					
	C	O	Ti	Na	Se	Cd
GCST1	15.10	40.58	29.45	0.83	3.65	10.40
GCST2	20.70	37.27	22.87	1.23	5.79	12.14
GCST3	25.30	31.02	19.94	1.28	8.37	14.09

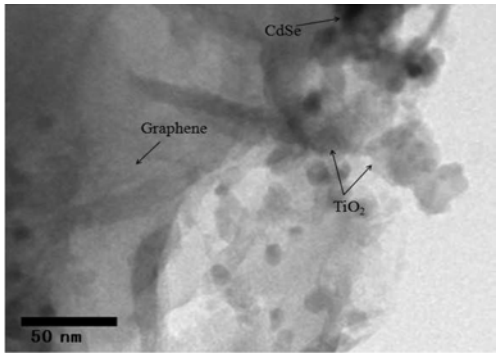

Fig. 3. TEM image of CdSe-graphene-TiO_2 composite.

for the different in the amount of graphene. For all of CdSe-graphene-TiO_2 composites, very uniform CdSe particles and TiO_2 particles can be observed. It can be difficultly found out the graphene flakes in sample GCST1 (Fig. 2 (a and b)), as there is small amount of graphene in the composites. However, for samples GCST2 and GCST3, the graphene flakes can be easily found out and the graphene flakes are decorated with the uniform CdSe particles and TiO_2 particles. It is reasonable to imagine that such a structure would enable easy charge transfer between the CdSe particles with TiO_2 particles and the graphene sheets.

The EDX elemental microanalysis (wt. %) of CdSe-graphene-TiO_2 composites shown in Table 2 indicates the presence of C, O, Ti, Cd, Se and Na. No other impure elements exited, indicates that the CdSe-graphene-TiO_2 composites with high purity has been successfully synthesized in this study. The C element should mainly originate from graphene sheets. The oxygen and Ti element mainly comes from the TiO_2 nanopowder. And the content of the carbon, Cd and Se element is increased with an order of GCST1, GCST2 and GCST3, which prepared by using an increasing of amount of graphene. This result is very agreed with XRD and SEM results.

More detailed information of the surface state and particle size were obtained by TEM (Fig. 3). The 2D structure of the graphene sheet and the surface was very smooth. Some of the graphenes are sutured together to form a large crumpled "paper". The TEM images of the nanocomposites distinctly reveal that CdSe, TiO_2 particles and agglomerates with diameters in the range of 30-60 nm are attached to the surface of grapheme

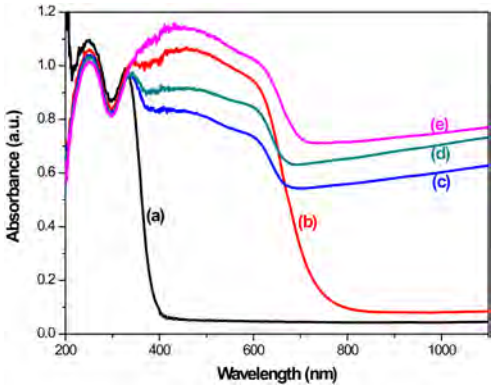

Fig. 4. UV-vis absorption spectra of pure TiO_2 (a), CdSe-TiO_2 (b), GCST1 (c), GCST2 (d) and GCST3 (e).

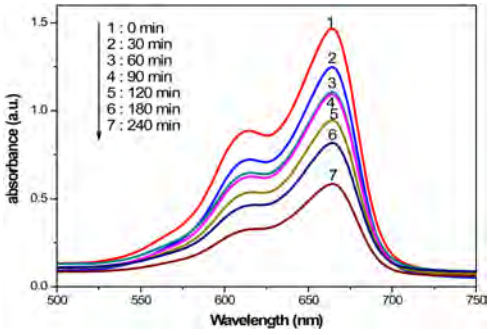

Fig. 5. Absorption spectra of MB solution (5×10^{-5} mol/L, 50 mL) in the presence of sample GCST3 composite (0.03 g) under exposure to visible light for 240 min.

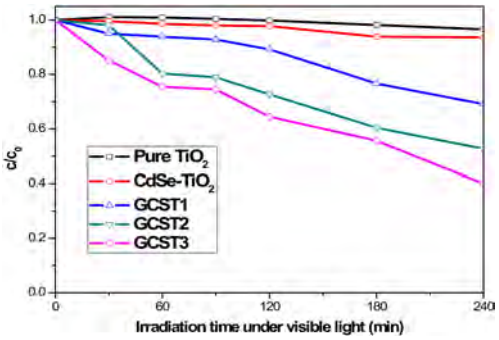

Fig. 6. Degradation of MB solution (5×10^{-5} mol/L, 50 mL) with different photocatalysts (0.03 g) under exposure to visible light for 240 min.

especially along the edges of the stacked nanosheets with thick-nesses of several nanometers. This implies that the compatibility between the CdSe, TiO_2 particles and graphene is good enough to obtain nano-sized dispersion without additional surface treatment.

Diffuse UV-vis reflectance data show that the pure TiO_2, CdSe-TiO_2 and CdSe-graphene-TiO_2 composites in Fig. 4. As expected, the spectrum obtained from the pure TiO_2 shows that TiO_2 absorbs mainly the ultraviolet light with absorption wavelength below 400 nm. After introducing of CdSe particles, the absorption edge is shifted toward the visible region and the absorption edge at approximately 738 nm. However, by combining with graphene sheets and CdSe particles, the CdSe-graphene-TiO_2 composites as-formed show an intense absorption and have a red-shift absorption onset comparing with both TiO_2 and CdSe-TiO_2. And the absorbance spectra are increased with an order of GCST1, GCST2 and GCST3, indicates the photocatalytic activity of CdSe-graphene-TiO_2 composites at high wavelength could be increased by increasing the amount of graphene. These phenomenon results not only from the excellent conductivity of graphene that can facilitate separation of photogenerated charges [29], but also from the introduction of the semiconductor quantum dot CdSe by which the conduction and valence bands of TiO_2 are bent downward [30].

Degradation of MB solution

To demonstrate the effect of graphene on the photocatalytic activity of CdSe-graphene-TiO_2 composites, the photocatalytic performance of CdSe-graphene-TiO_2 composites was studied for the degradation of MB in water. The characteristic absorption peak of MB solution at 665 nm was chosen as the monitored parameter to detect the concentration of MB. Fig. 5 shows the evolution if absorption spectra of MB in the presence of 0.03 g sample GCST3 composite, from which we can clearly see that the intensity of the adsorption peaks corresponding to MB gradually diminish with increasing irradiation time. Fig. 5 shows the change in the concentration of MB with different irradiation time in the presence of different photocatalysts, from which we can obviously see that the pure TiO_2 has almost no photocatalytic activity toward the photodegradation of MB solution. The MB solution degraded a little even introducing of CdSe particles. However, for CdSe-graphene-TiO_2 composites, a much excellent photocatalytic activity toward the photodegradation of MB can be seen from the Fig. 6. And the photocatalytic activity toward the photodegradation of MB is increased by increasing the amount of graphene in composites.

Photocatalytic reactions on different photocatalysts can be expressed by the Langmuir-Hinshelwood model [31]. The photocatalytic degradation of MB containing different photocatalysts under visible light obeys pseudo-first-order kinetics with respect to the concentration of MB:

$$-dc/dt = k_{app}c$$

Integration of equation (with the restriction of $c = c_0$ at $t = 0$, with the c_0 being the initial concentration in the bulk solution after dark adsorption and t the reaction time) will lead to the following expected relation:

$$-\ln(c/c_{ads}) = k_{app}t$$

where c and c_0 are the reactant concentration at time $t = t$ and $t = 0$, respectively, k_{app} and t are the apparent reaction rate constant and time, respectively. According

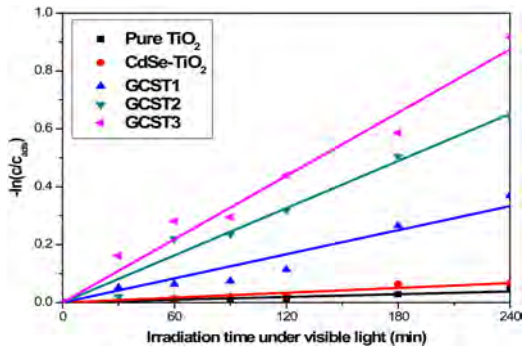

Fig. 7. Variations in -ln(c/c_{ads}) as a function of irradiation time and linear of different photocatalysts on the degradation of MB solution under irradiation of visible light for 240 min at room temperature.

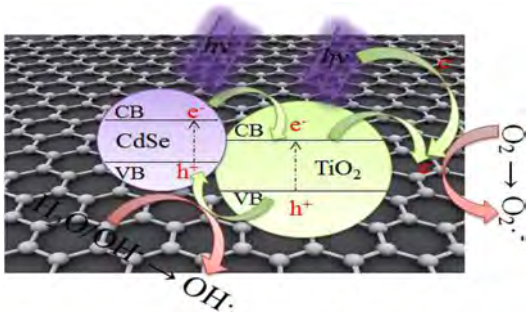

Fig. 8. The scheme of excitation and charge transfer process between TiO_2 particles, CdSe particles and graphene sheests.

Table 3. kinetics parameters of photocatalytic degradation of MB at different samples

Samples	k_{app} (min^{-1})	R
TiO_2	1.6×10^{-4}	1
CdSe-TiO_2	2.8×10^{-4}	1.75
GCST1	1.4×10^{-3}	8.75
GCST2	2.7×10^{-3}	16.88
GCST3	3.6×10^{-3}	22.5

to the equation, a plot of -ln(c/c_{ads}) versus t will yield a slope of k_{app}. The results are displayed in Fig. 7 and also summarized in Table 3. The MB degradation rate constant for CdSe-graphene-TiO_2 composites reaches 1.4×10^{-3} min^{-1}, 2.7×10^{-3} min^{-1} and 3.6×10^{-3} min^{-1} for samples GCST1, GCST2 and GCST3, respectively, which greatly higher than both of pure TiO_2 and CdSe-TiO_2. The above results suggest the CdSe-graphene-TiO_2 composites are much more effective photocatalyst. The high activity can be attributed to the synergetic effects of high charge mobility, and red shift in absorption edge of CdSe-graphene-TiO_2 composites.

The scheme of excitation and charge transfer process between CdSe and TiO_2 under light irradiation is shown in Fig. 8. Under irradiation by visible lamp, both CdSe and TiO_2 can be excited (corresponding to Eq. (1) and (2), respectively), the generated electrons in CdSe and holes in TiO_2 are then immigrated to the conduction band (CB) of TiO_2 and the valence band (VB) of CdSe, respectively. This transfer process is thermodynamic favorable due to both the CB and VB of CdSe lie above that of TiO_2. In addition, graphene nanosheets acting as good electron acceptors [32, 33] can accept the electrons by light irradiation and the electrons exited in CB of TiO_2 are also transferred to the surface of graphene (Eq. (3) and (4)). Thus the lifetime of the excited electrons (e^-) and holes (h^+) is prolonged in the transfer process, inducing higher quantum efficiency. Meanwhile, the generated electrons probably react with dissolved oxygen molecules and produce oxygen peroxide radical $O_2^{\bullet-}$ (Eq. (5), (6) and (7)), the positive charged hole (h^+) may react with the OH^- derived from H_2O to form hydroxyl radical $OH^\bullet$ (Eq. (8) and (9)). The MB molecule then can be photocatalytically degraded by oxygen peroxide radical $O_2^{\bullet-}$ and hydroxyl radical $OH^\bullet$ to CO_2, H_2O and other mineralization (Eq. (10)).

$$CdSe + h\nu \rightarrow CdSe(e^-) + CdSe(h^+) \quad (1)$$
$$TiO_2 + h\nu \rightarrow TiO_2(e^-) + TiO_2(h^+) \quad (2)$$
$$Graphene + h\nu \rightarrow Graphene(e^-) \quad (3)$$
$$TiO_2(e^-) + Graphene \rightarrow Graphene(e^-) + TiO_2 \quad (4)$$
$$CdSe(e^-) + O_2 \rightarrow CdSe + O_2^{\bullet-} \quad (5)$$
$$TiO_2(e^-) + O_2 \rightarrow TiO_2 + O_2^{\bullet-} \quad (6)$$
$$Graphene(e^-) + O_2 \rightarrow Graphene + O_2^{\bullet-} \quad (7)$$
$$CdSe(h^+) + H_2O \rightarrow CdSe + OH^\bullet + H^+ \quad (8)$$
$$TiO_2(h^+) + H_2O \rightarrow TiO_2 + OH^\bullet + H^+ \quad (9)$$
$$O_2^{\bullet-} \text{ or } OH^\bullet + MB \rightarrow CO_2, H_2O \text{ and other mineralization} \quad (10)$$

Conclusions

CdSe-graphene-TiO_2 composites were prepared by a simple hydrothermal method by using grapheme oxide, CdSe and TiO_2 nanopowder. Typical anatase TiO_2 structure and cubic CdSe structure can be observed in XRD patterns of all of CdSe-graphene-TiO_2 composites. From the SEM morphology, for samples GCST2 and GCST3, the graphene flakes can be easily found out and the graphene flakes are decorated with the uniform CdSe particles and TiO_2 particles. And the content of the carbon is increased with an order of GCST1, GCST2 and GCST3, which prepared by using an increasing of amount of graphene. The CdSe-graphene-TiO_2 composites show an intense absorption and have a red-shift absorption onset comparing with both TiO_2 and CdSe-TiO_2. And the absorbance spectra are increased with an order of GCST1, GCST2 and GCST3. The MB degradation results suggest the CdSe-graphene-TiO_2 composites are much more effective photocatalyst than pure TiO_2 and CdSe-TiO_2. The high activity can be attributed to the synergetic effects of high charge mobility, and red shift in absorption edge of CdSe-graphene-TiO_2 composites.

References

1. K. Hashimoto, H. Irie and A. Fujishima, Jpn. J. Appl. Phys. 44 (2005) 8269-8285.
2. A.L. Linsebigler, G.Q. Lu and J.T. Yates, Chem. Rev. 95 (1995) 735-758.
3. K. Kawasaki, D. Yamazaki, A. Kinoshita, H. Hirayama, K. Tsutsui and Y. Aoyagi, Appl. Phys. Lett. 79 (2001) 2243-2248.
4. T.R. Nielsen, P. Gartner and F. Jahnke, Phys. Rev. B 69 (2004) 235314-235319.
5. M.T. Todaro, M. De Giorgi, V. Tasco, M. De Vittorio, R. Cingolani and A. Passaseo, Appl. Phys. Lett. 84 (2004) 2482-2486.
6. Z. Ye, J.C. Campbell, Z. Chen, E.-T. Kim and A. Madhukar, J. Appl. Phys. 92 (2002) 7462-7468.
7. L.M. Peter, D.J. Riley, E.J. Tull and K.G.U. Wijayantha, Chem. Commun. Cambridge (2002) 1030-1031.
8. Q. Shen, D. Arae and T. Toyoda, J. Photochem. Photobiol. A 164 (2004) 75-80.
9. A.J. Nozik, Physica E-Amsterdam 14 (2002) 115-120.
10. R. Schaller and V.I. Klimov, Phys. Rev. Lett. 92 (2004) 186601-186604.
11. P. Yu, K. Zhu, A.G. Norman, S. Ferrere, A.J. Frank and A.J. Nozik, J. Phys. Chem. B 110 (2006) 25451-25457.
12. I. Robel, V. Subramanian, M. Kuno and P.V. Kamat, J. Am. Chem. Soc. 128 (2006) 2385-2389.
13. R. Plass, S. Pelet, J. Krueger and M. Gratzel, J. Phys. Chem. B 106 (2002) 7578-7583.
14. Zhu L, Meng Z D, Chen M L, Zhang F J, Choi J G, Park J Y and Oh W C. J Photocataly Sci, 2010, 1:69.
15. H. Zhang, X. Lv, Y. Li, Y. Wang and J. Li, ACS Nano. 4 (2010) 380-386.
16. S.R. Kim, M.K. Parvez and M. Chhowalla, Chem. Phys. Lett. 483 (2009) 124-127.
17. G.M. Scheuermann, L. Rumi, P. Steurer, W. Bannwarth and R. Mulhaupt, JACS 131 (2009) 8262-8270.
18. R. Pasricha, S. Gupta and A.K. Srivastava, Small 5 (2009) 2253-2259.
19. R. Muszynski, B. Seger and P.V. Kamat, J. Phys. Chem. C 112 (2008) 5263-5266.
20. T.N. Lambert, C.A. Chavez, B. Hernandez-Sanchez, P. Lu, N.S. Bell, A. Ambrosini, T. Friedman, T.J. Boyle, D.R. Wheeler and D.L. Huber, J. Phys. Chem. C 113 (2009) 19812-19823.
21. Y. Lin, K. Zhang, W. Chen, Y. Liu, Z. Geng, J. Zeng, N. Pan, L. Yan, X. Wang and J.G. Hou, ACS Nano. 4 (2010) 3033-3038.
22. W.C. Oh, M.L. Chen, K. Zhang, F.J. Zhang and W.K. Jang, J. Korean Phys. Soc. 56 (2010) 1097-1102.
23. W.C. Oh and F.J. Zhang, Asian J. Chem. 23 (2011) 875-879.
24. M.L. Chen, C.Y. Park, J.G. Choi and W.C. Oh, J. Kor. Cera. Soc. 48 (2011) 147-151.
25. W.C. Oh, J.S. Bae and M.L. Chen, Bull. Kor. Chem. Soc. 27 (2006) 1423-1328.
26. M.L. Chen, F.J. Zhang, K. Zhang, Z.D. Meng and W.C. Oh, J. Photocatal. Sci. 1 (2010) 19-28.
27. T.T. Wang, J.L. Wang, Y.C. Zhu, F. Xue, J. Cao and Y.T. Qian, J. Phys. Chem. Solids 71 (2010) 940-945.
28. A.E. Raevskaya, A.L. Stroyuk, S.Ya. Kuchmiy, Yu.M. Azhniuk, V.M. Dzhagan, V.O. Yukhymchuk and M.Ya. Valakh, Colloids and Surfaces A: Physicochem. Eng. Aspects 290 (2006) 304-309.
29. N.L. Yang, J. Zhai, D. Wang, Y.S. Chen and L. Jiang, ACS Nano 4 (2010) 887-894.
30. W.K. Ho and J.C. Yu, J. Mol. Catal. A: Chem. 247 (2006) 268-274.
31. Y. Li, X. Li, J. Li and J. Yin, Water Research 40 (2006) 1119-1126.
32. G. Williams, B. Seger and P.V. Kamat, ACS Nano 2 (2008) 1487-1491.
33. I.V. Lightcap, T.H. Kosel and P.V. Kamat, Nano Lett. 10 (2010) 577-583.